MINX Document 5
Measuring Aerosol Height and Motion

David Nelson, Ralph Kahn, Michael Tosca, Sebastian Val,
Michael Garay, and MISR Staff

Jet Propulsion Laboratory, California Institute of Technology,
Raytheon Company and Columbus Technologies and Services, Inc.

April, 2015

Contents

- Parallax, disparity and image matching
- Height/wind retrieval algorithm
- MINX height retrieval comparisons

Parallax

Parallax is a difference in the apparent position of an object viewed along different lines of sight. Objects nearer the viewer have larger parallax than more distant objects, so parallax can be used to determine distance.

In this example, each of MISR's 9 cameras views a stationary cloud from a different angle at a different time

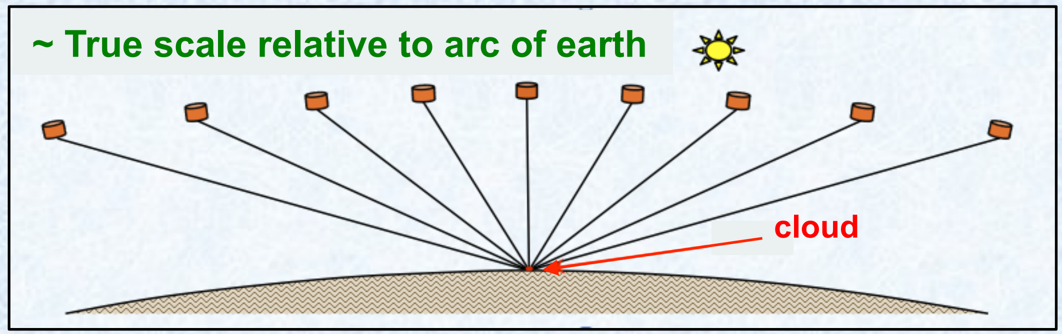

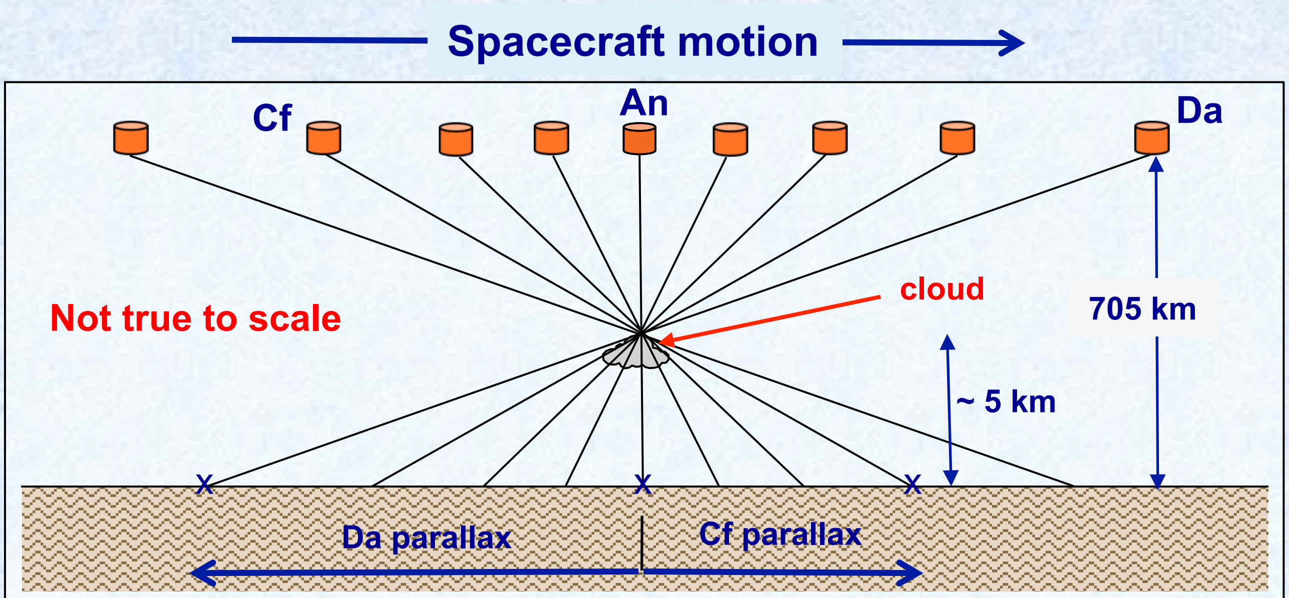

This shows how Da and Cf camera parallax are measured relative to the An reference camera

Note that a point on the ground would have no parallax

Disparity - 1

Disparity is closely related to parallax. It is the measure of total offset in the apparent position of an object relative to the surface, when viewed along different lines-of-sight, due to the combination of height parallax and any actual movement of the object between views. In MINX, the direction of cloud (or plume) motion, but not the speed of motion, is input by the user.

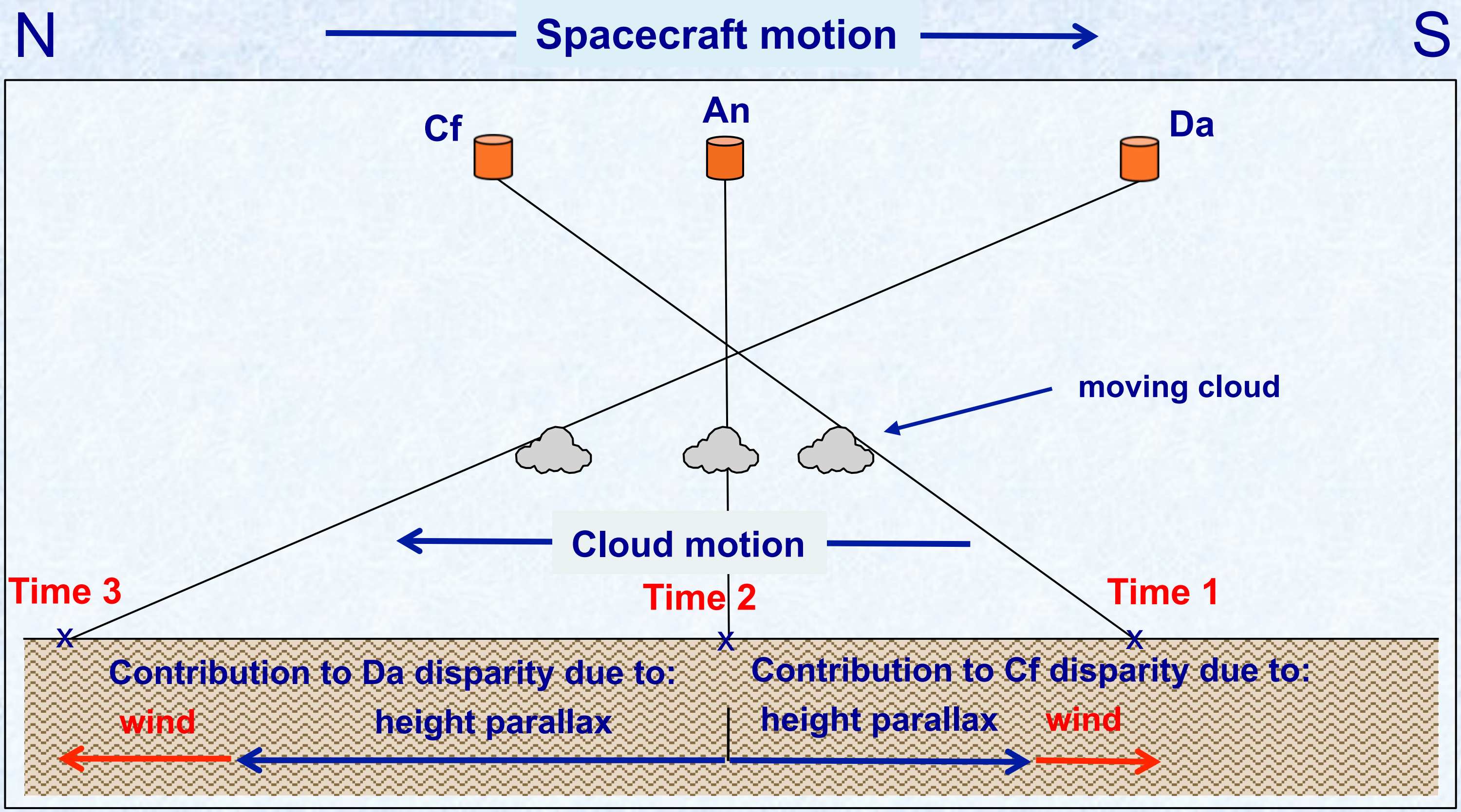

Cloud motion in direction opposite spacecraft motion

Disparity - 2

If the entire disparity is attributed to height parallax (zero-wind height) when the object actually moved between views, then:

- **For cloud and spacecraft motion in the same direction, the height estimate will be too low**
- **For cloud and spacecraft motion in opposite directions, the height estimate will be too high**

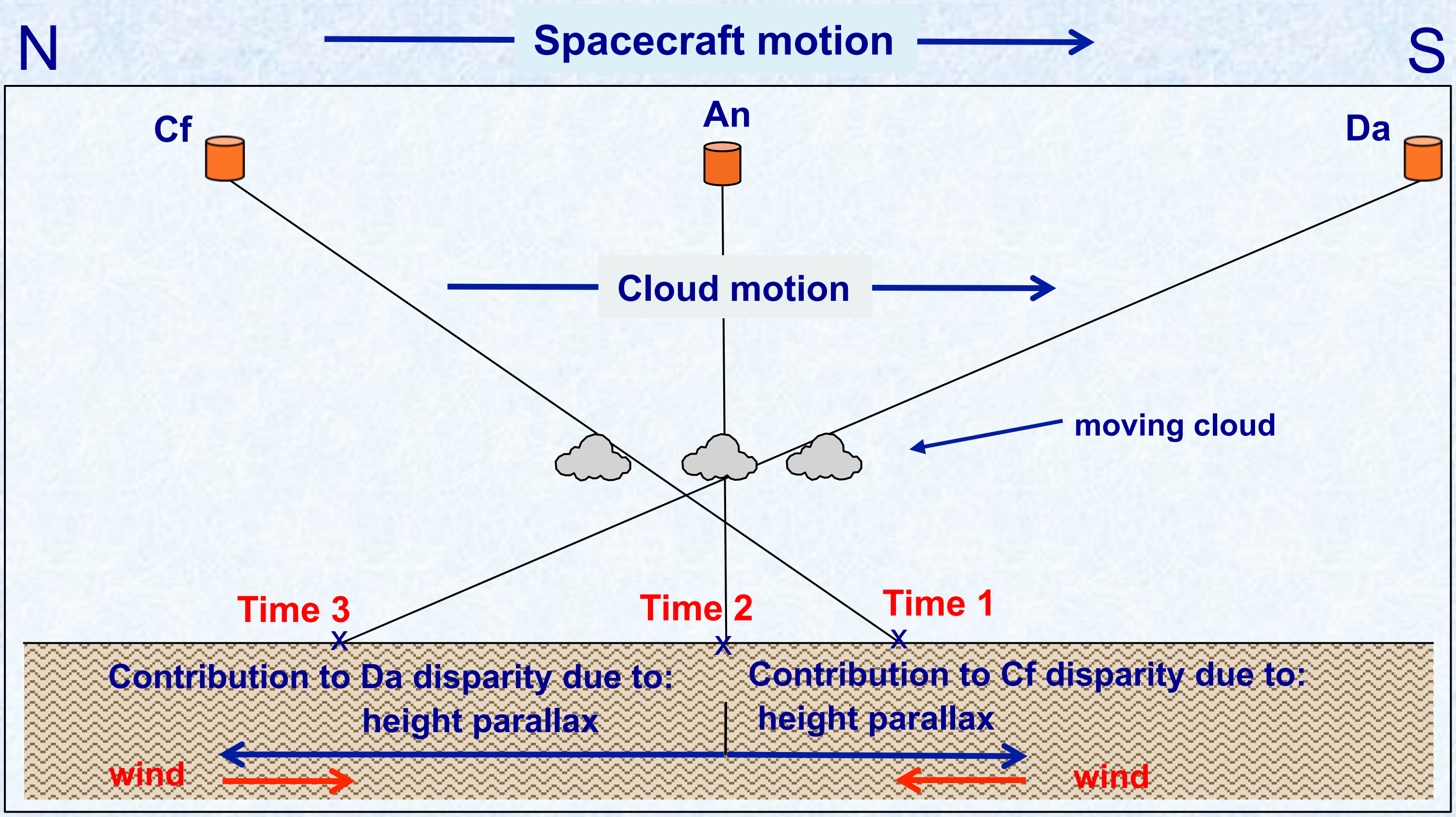

Cloud motion in same direction as spacecraft motion

Image Matching - 1

Objective: To find a feature in the image from a non-nadir camera that corresponds to a feature in the image from the An camera and to measure its disparity.

Reference image Comparison image

Alaska fire with small pyrocumulus clouds showing effect of parallax (plus motion due to wind?)

- In MINX, the An camera always acts as the reference image
- Six or eight of the other MISR cameras provide comparison images
- Image matching finds disparities between the target pixel location in the reference image and the corresponding pixel location in the comparison image
- Disparity has across-track (left-right) and along-track (up-down) components in the Space-Oblique Mercator (SOM) projection that MISR uses
- Image matching can be applied to features on <u>or</u> above the earth's surface
- MINX uses the correlation coefficient (CC) for assessing the quality of a match
- Image-matching will fail if the images lack texture or distinctive features

Image Matching - 2

Correlation Coefficient: $$r_{xy} = \frac{\sum (x_i - \bar{x})(y_i - \bar{y})}{(n-1)s_x s_y}$$

Where:

r_{xy} = correlation coefficient
x_i = BRF values at pixels in reference patch
$\bar{x}$ = mean value of the BRFs in reference patch
y_i = BRF values at pixels in comparison patch
$\bar{y}$ = mean value of the BRFs in comparison patch
n = number of pixels in reference patch
s_x = standard dev. of BRF values in reference patch
s_y = standard dev. of BRF values in comparison patch

(BRF is Bidirectional Reflectance Factor)

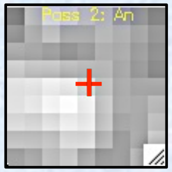

An red-band reference patch

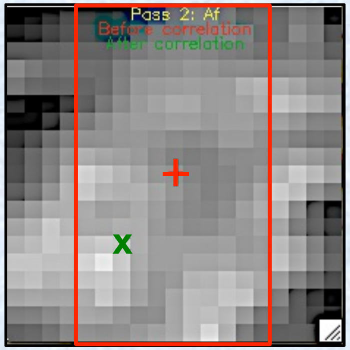

Af red-band search region (red rectangle)

MINX reference patch from An image and search region from Af comparison image - the red + is the target pixel and the green x is solution pixel with highest correlation

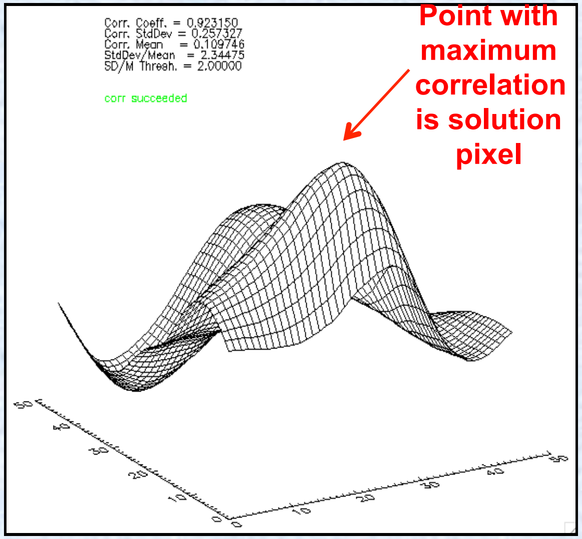

Correlation matrix interpolated to obtain sub-pixel resolution

- Correlation finds match to nearest pixel
- To increase precision, fit a bi-cubic surface to the correlation matrix around the solution pixel and interpolate to derive a finer grid
- Find the fine grid point with the largest CC - this gives fractional (sub-pixel) disparities

Image Matching - 3

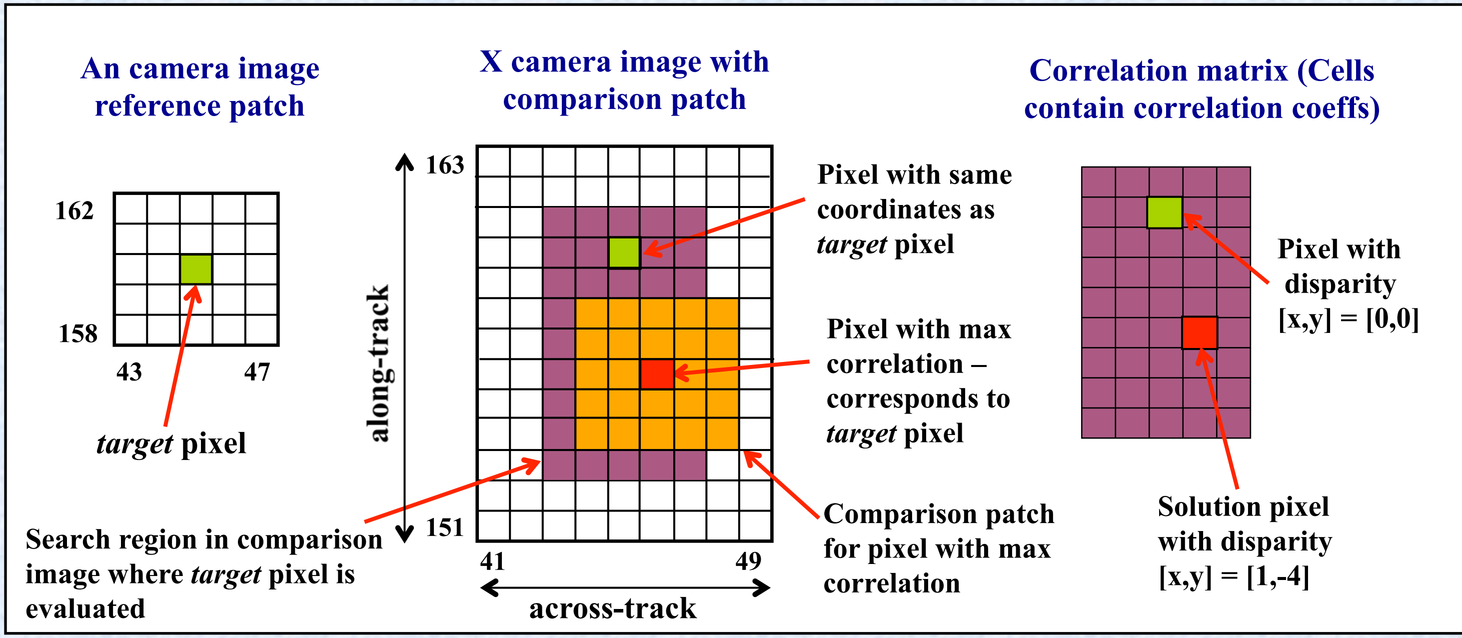

Violet area is the search region where corresponding pixel is expected to be, based on calculations using maximum allowed height and wind speed

① **Center the target pixel of the reference patch over the upper-left-most pixel in the comparison image's search region**

② **Calculate a correlation coefficient using BRFs for the overlapping pixels and place results into its corresponding location in correlation matrix**

③ **Move the reference patch to next pixel in search region and compute CC again – repeat for all pixels in search region (45 positions in this example)**

④ **The pixel in the comparison image with highest CC is the match**

Contents

- Parallax, disparity and image matching
- Height/wind retrieval algorithm
- MINX height retrieval comparisons

MINX Top Level Height/Wind Retrieval Algorithm

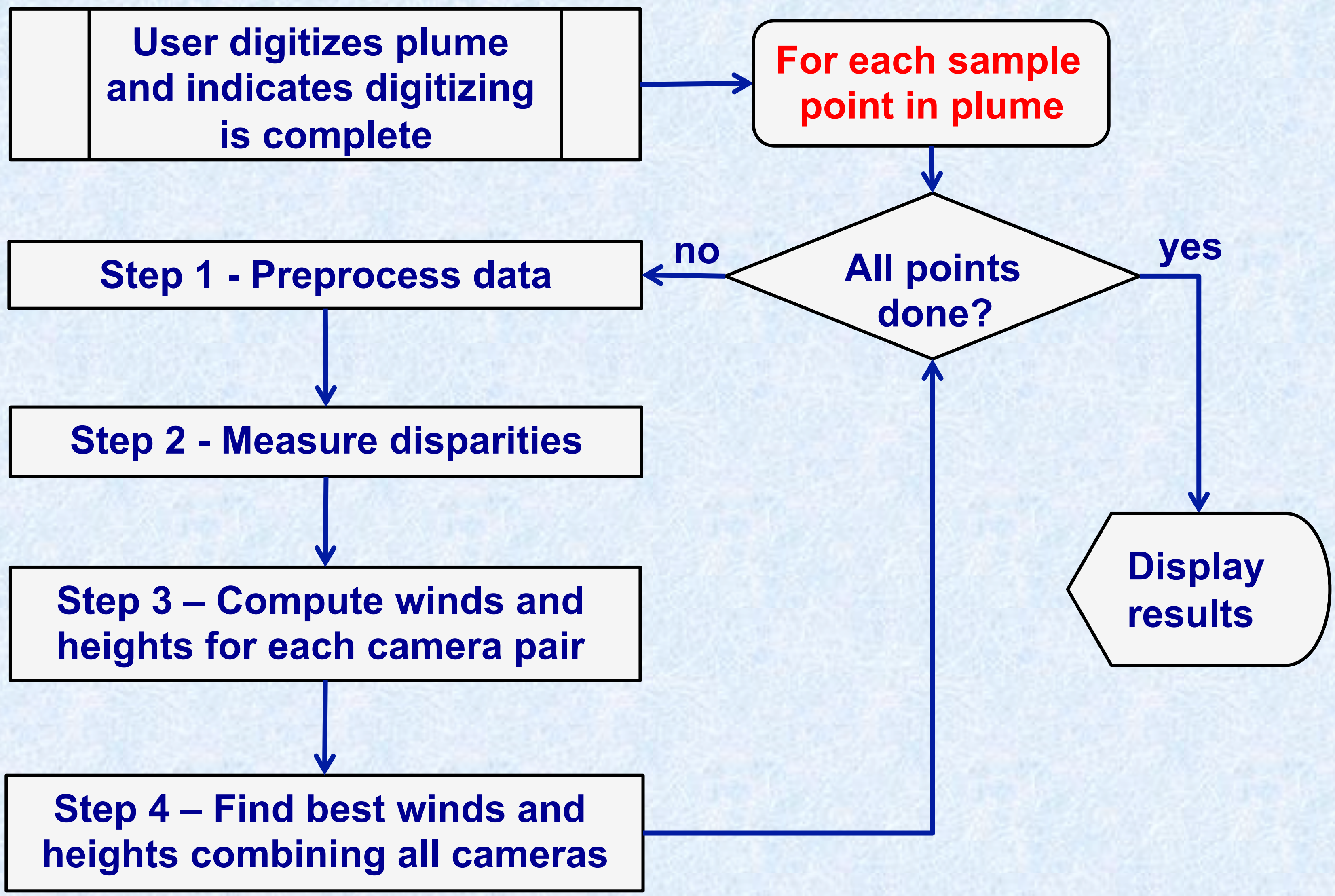

Step 1 - Preprocess Data

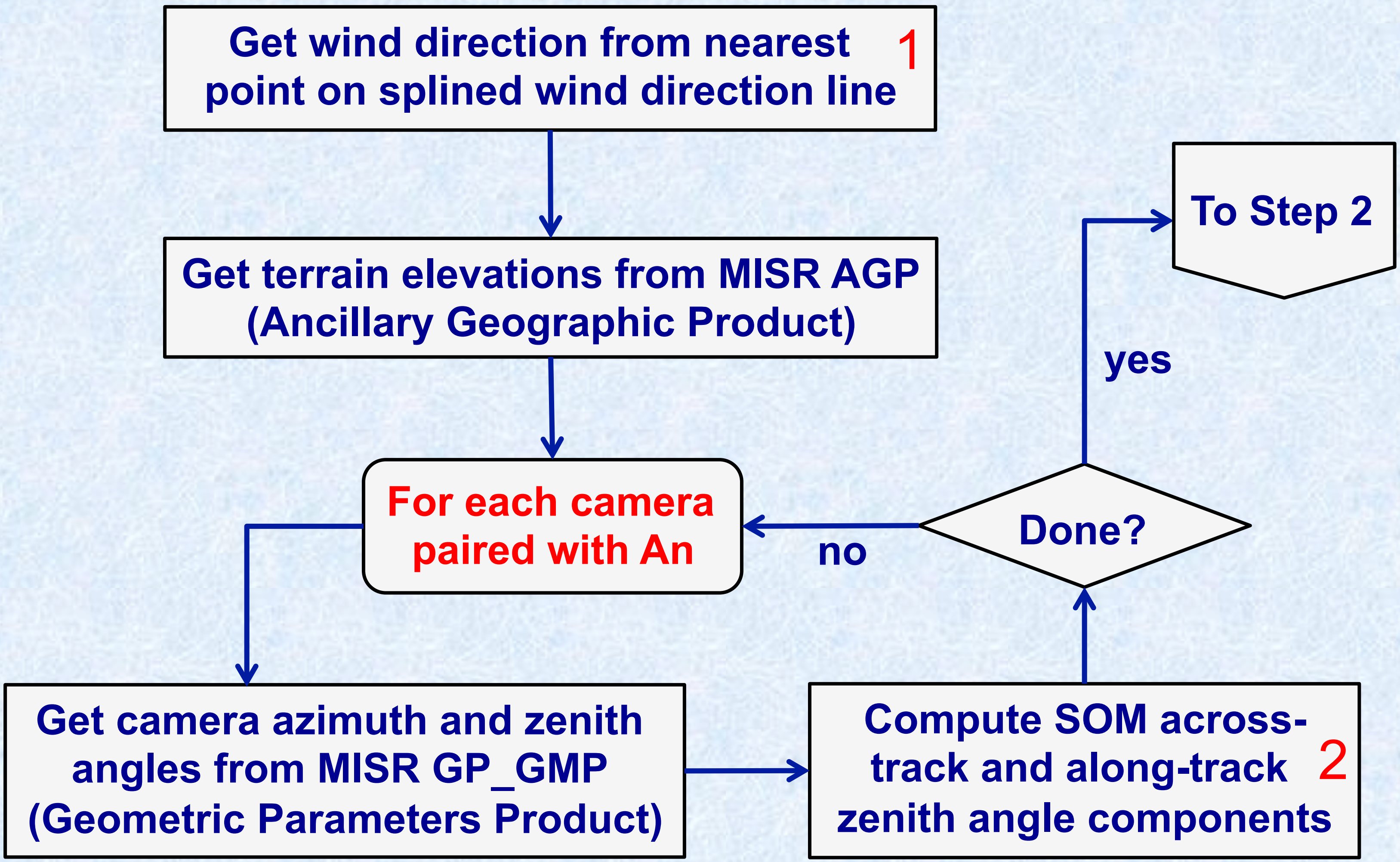

1 - Get Wind Direction

- The height/wind retrieval problem has 3 unknowns : height, wind-speed across-track and wind-speed along-track
- The user inputs a (wind) direction of motion during digitizing
- If either the across-track or the along-track wind speed is known, the other component can be computed using the wind direction
- So the retrieval problem simplifies to 2 unknowns for each camera pair

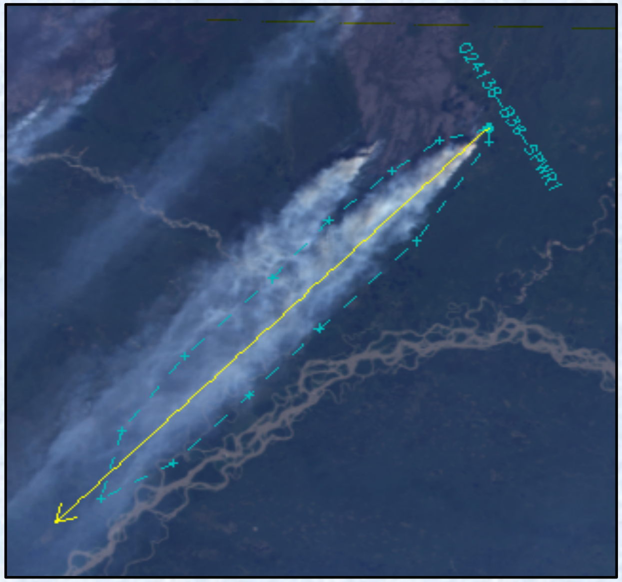

Digitized plume showing "wind direction" line in yellow

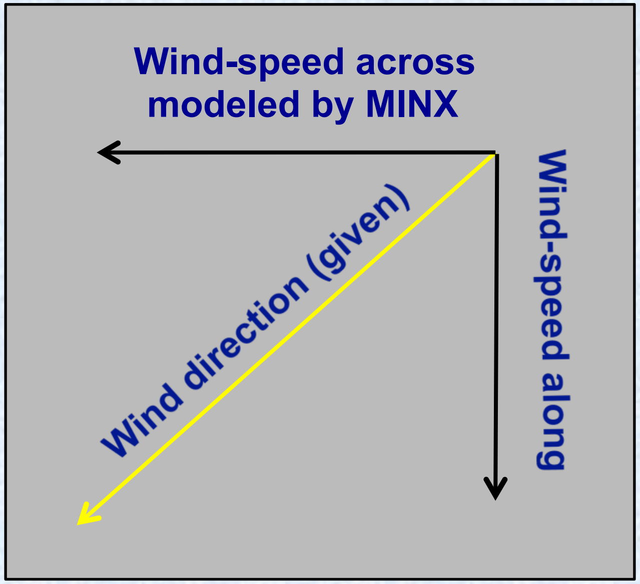

Wind-speed along-track is easily computed from wind-speed across-track plus wind direction

2 - Compute Across and Along-Track Zenith Angles

Objective: To convert camera azimuth and camera zenith angles to 2 orthogonal components of zenith angle in the SOM across-track and along-track directions. This allows us to compute the 2 components of disparity independently.

① **Create a closely spaced pair of points P1 = [lat1, long] and P2 = [lat2, long] on the same geographic meridian in the region of interest, and project each to SOM coordinates**

② **Find distances (dx_{north} , dy_{north}) along the SOM_{north} and SOM_{east} axes between the points**

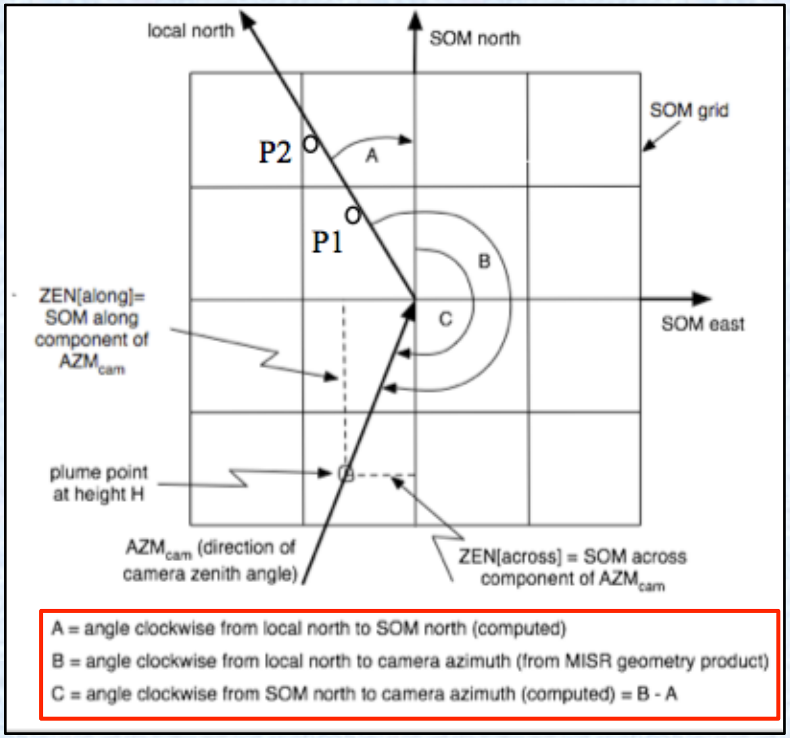

③ **Compute the angle, *A*, clockwise from local north to SOM_{north}: $A = ATAN(dx_{north}, dy_{north})$**

④ **Compute the angle, C, clockwise from SOM_{north} to the azimuth direction of the camera (AZM_{cam}) to give the SOM-relative azimuth angle of the camera (AZM_{som}): $C = B - A$**

⑤ **Decompose the camera zenith angle (ZEN_{cam}) into across-track and along-track components to derive the SOM zenith angles (ZEN_{som}):**

$$ZEN_{SOM}[across] = ZEN_{CAM} * SIN(AZM_{SOM})$$

$$ZEN_{SOM}[along] = ZEN_{CAM} * COS(AZM_{SOM})$$

Step 2 – Measure Disparities

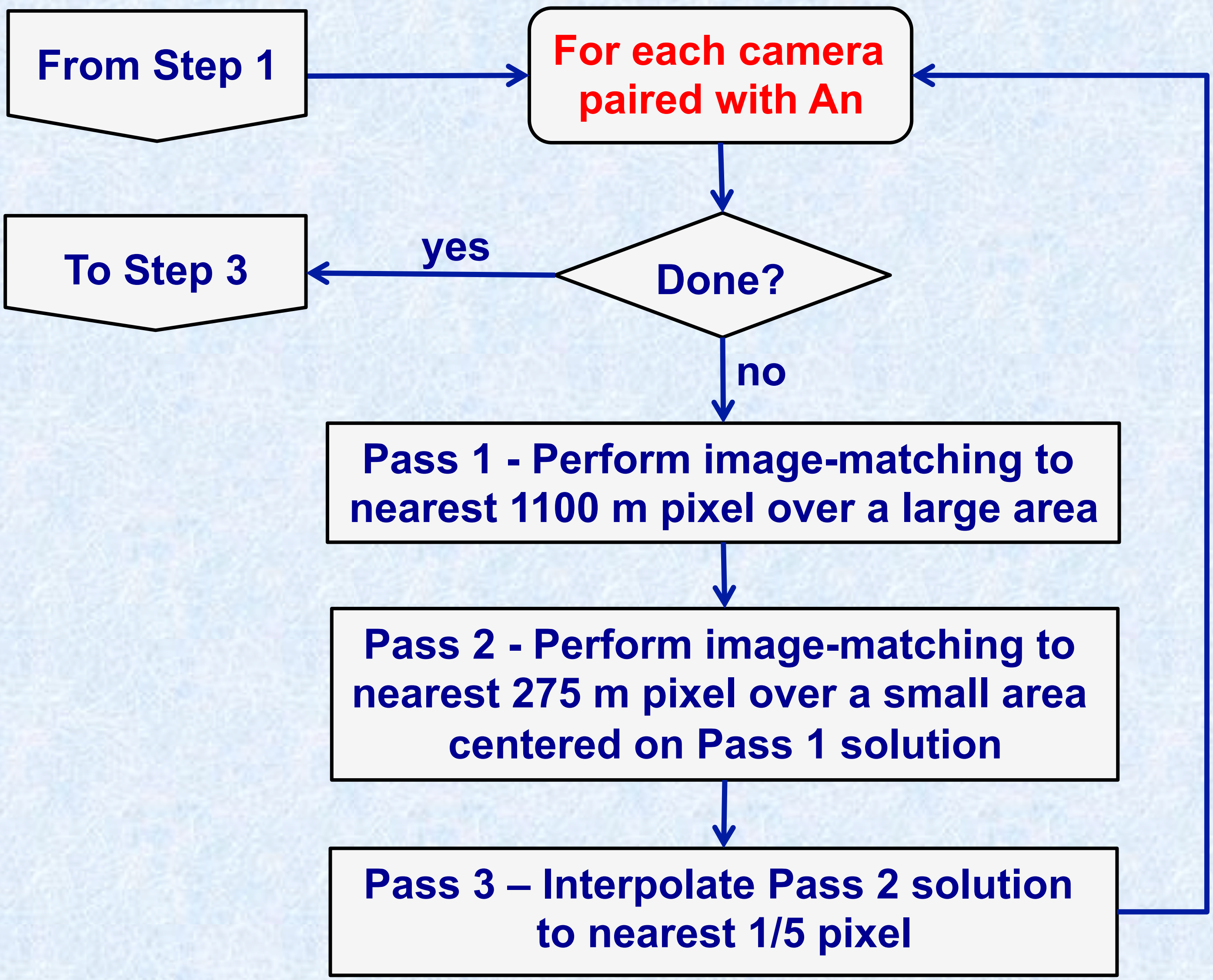

Step 3 – Compute Winds and Heights for Each Camera Pair

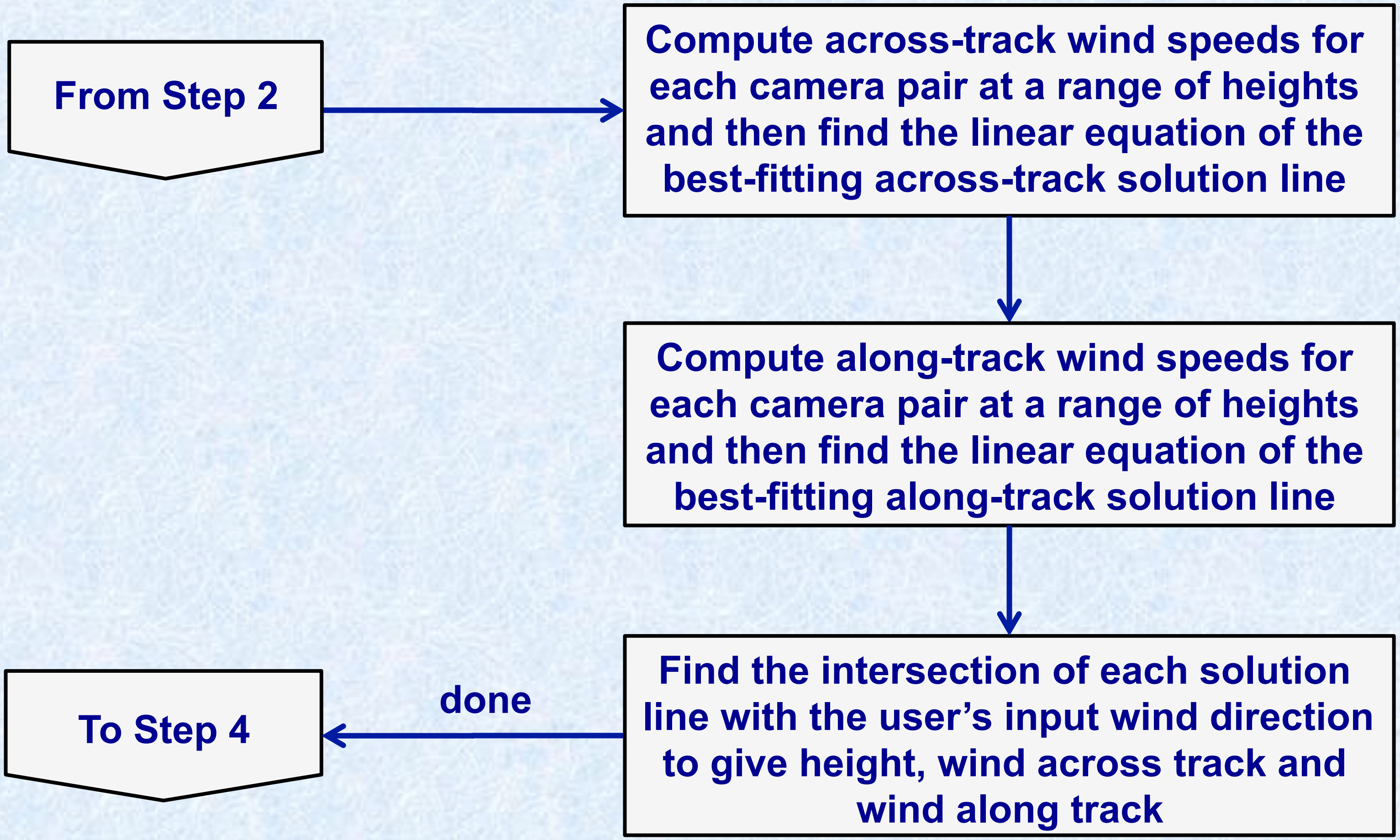

3D Data Cube of Disparity Differences and the Solution Line

- Each node in the data array is indexed by model parameters X (wind-speed across), Y (wind-speed along) and H (height)
- Each node contains a disparity difference: $D_{total} = D_{measured} - D_{modeled}$
- Best height/wind solutions exist wherever $D_{total} = 0$; this is true for all points on a sloping line parallel to the wind-speed along axis
- The intersection of this line with a plane containing the user-supplied wind direction is the solution

If wind direction is known, the analysis needs to be done only in the plane containing the wind direction - 3 unknowns reduce to 2 and a camera pair rather than a camera triplet is able to provide a unique solution

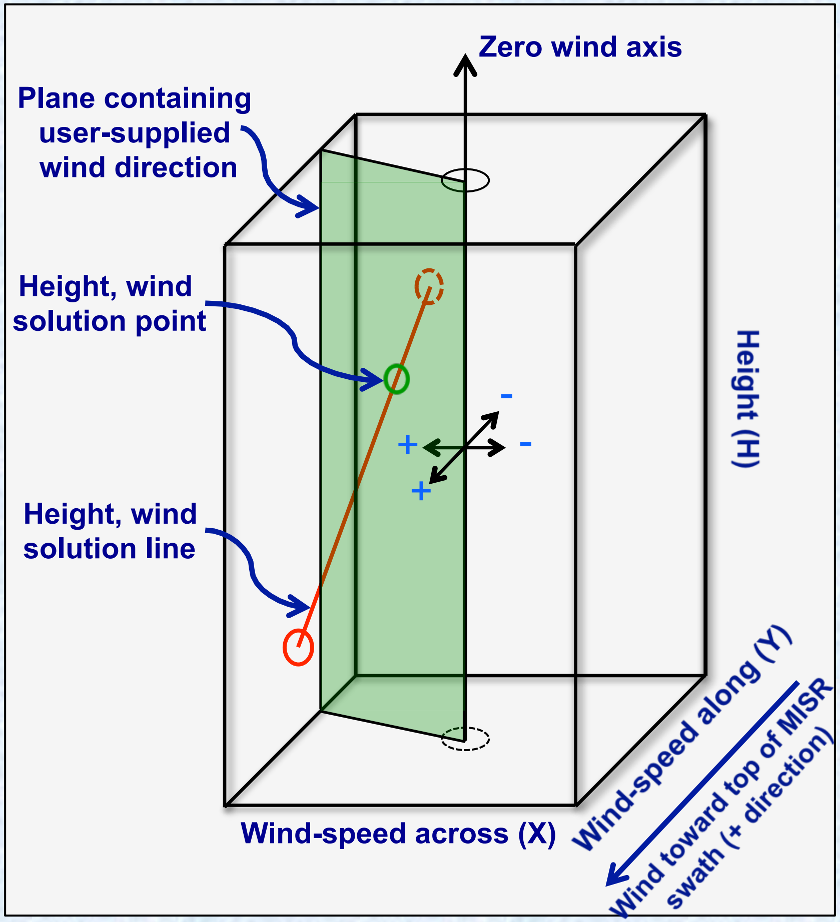

3D data array for solution of winds and height for one camera at one data point

Step 4 – Find Best Height and Winds Combining all Successful Cameras

From Step 3

Find median values of the heights and the winds from all cameras with successful retrievals

Keep all camera solutions whose heights and winds differ from the medians by less than some threshold values

If at least 3 (or 2) camera solutions remain, consider retrieval successful, so find the means of the remaining heights and winds and report them

Done – on to next point

The actual method more closely resembles a quasi-cluster-analysis algorithm with height- or wind speed-dependent thresholds

MISR vs. MINX Stereo Height Algorithms

Feature	MISR Standard Stereo Product	MINX
Level 1 imagery	Ellipsoid-projected	Terrain-projected
Matcher cost func	Mean of normalized differences	Pearson's correlation coefficient
Order of solution	Winds retrieved first, heights later	Winds and heights retrieved simultaneously
Cameras used	An / Bx / Dx triplets for wind Af / An / Aa triplets for height	Cf, Bf, Af, Aa, Ba, Ca, each paired with An for height and wind
Wind retrieval dependency	Depends on earth curvature viewed by D cameras, is automatic and is applicable to any feature above terrain	Depends on knowledge of wind direction and is generally applicable where user can input a known wind direction
Wind resolution	Wind retrievals averaged over 70.4 km and applied to heights at 1.1 km	Heights and winds retrieved simultaneously at 1.1 km resolution
Number of unknowns	3: wind speed across-track, wind speed along-track and height	2: one wind speed plus height; the other wind speed is derived from a user-supplied wind direction
Methodology	Finds unique inverse solution using 1 set of camera triplets (2 sets for wind)	Finds inverse solution that averages results from up to 8 camera pairs

Contents

- Parallax, disparity and image matching
- Height/wind retrieval algorithm
- MINX height retrieval comparisons

Height Retrieval Comparison – MINX and MISR Standard Stereo Height Product (TC_STEREO)

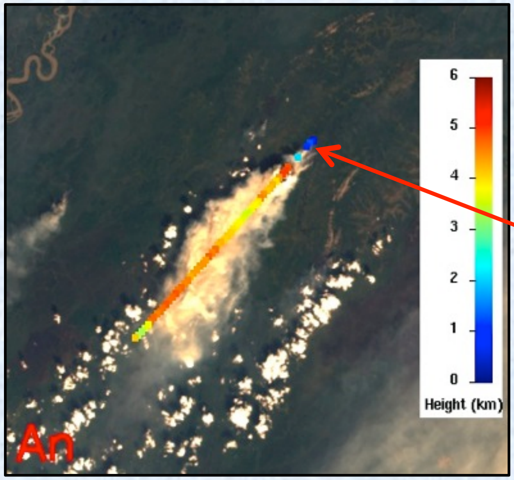

- MINX and MISR zero-wind and wind-corrected heights are similar
- MISR heights and winds are "quantized" due to matching at whole pixel level
- MISR winds are constant over large distances due to 70.4 km resolution retrieval
- Across-track winds are more similar than along-track winds
- The TC_CLOUD version of the MISR stereo product introduced in 2014 produces improved results compared to earlier versions

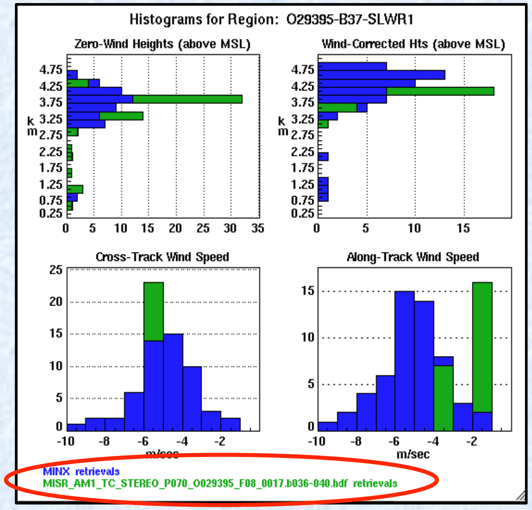

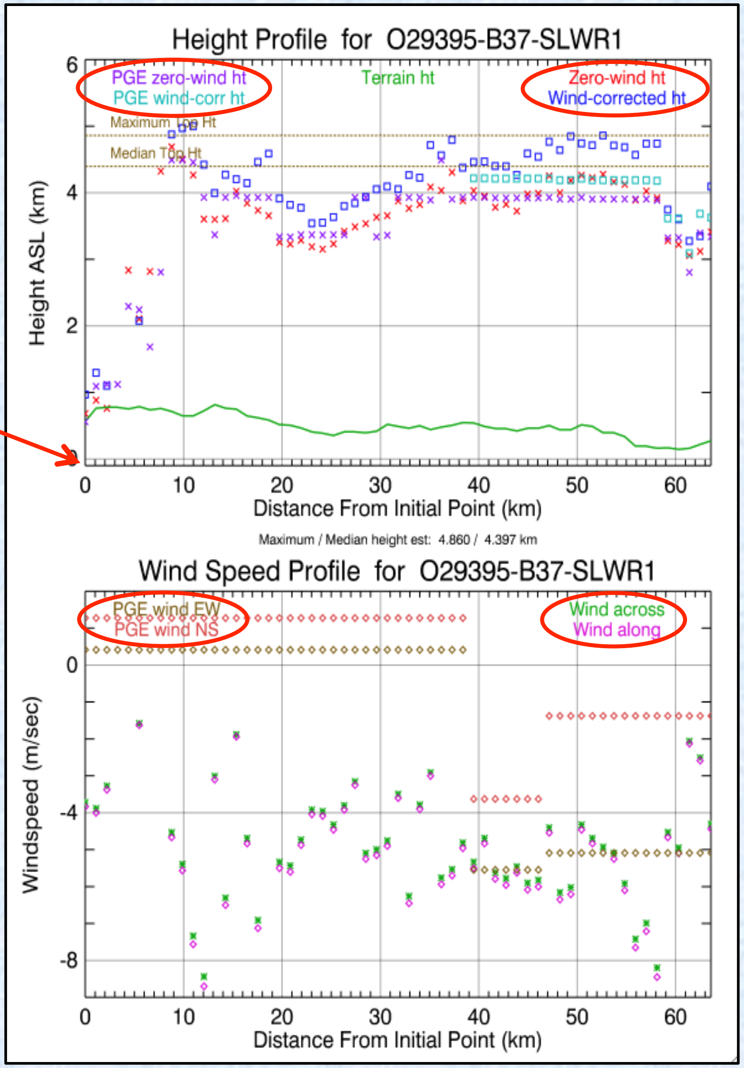

Height Retrieval Comparison – MINX and Temperature-Retrieved Heights and other Sources

MINX plume heights for 8 Ring of Fire volcanic eruptions compared with heights from other sources

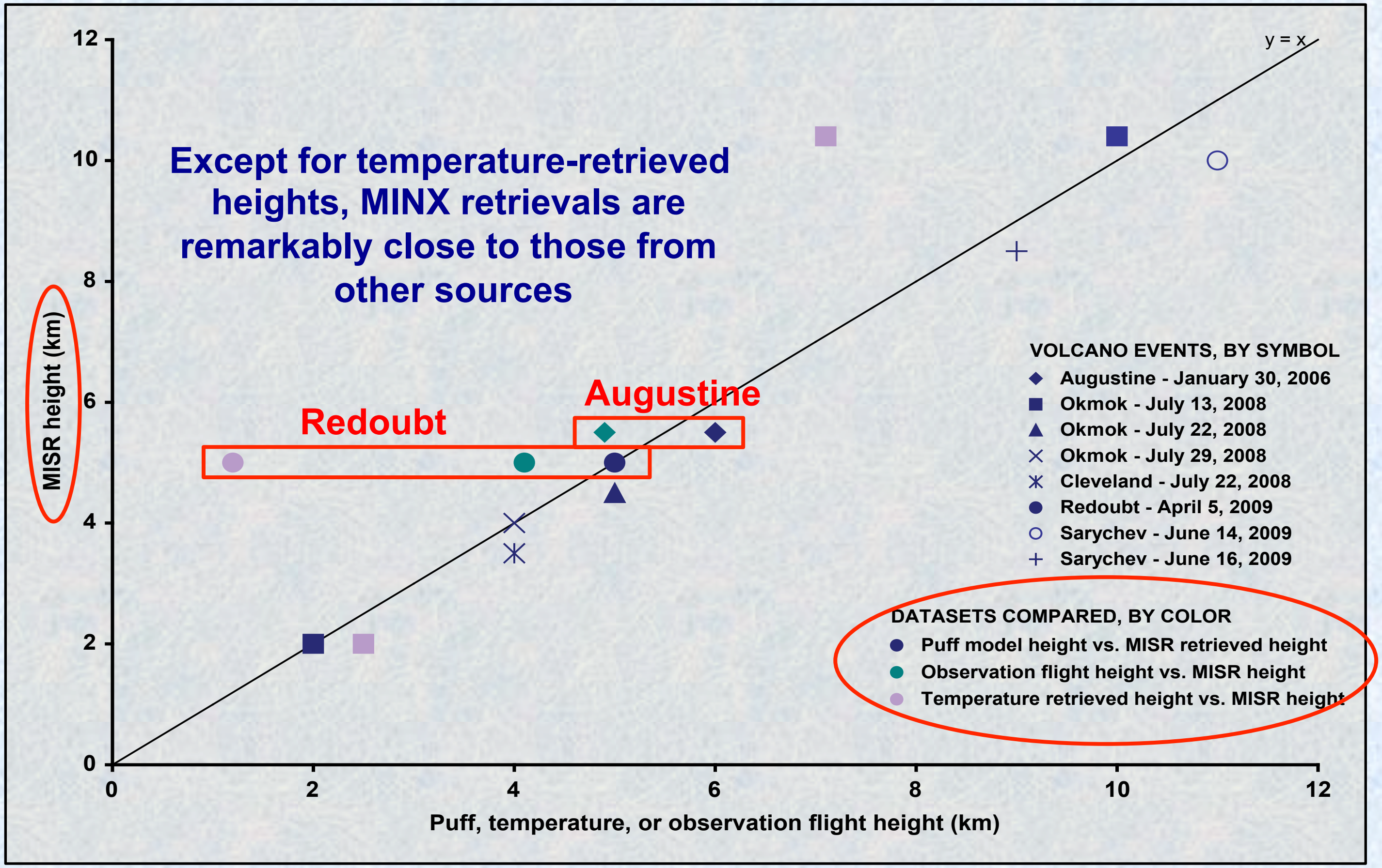

Courtesy of Angela Ekstrand, Alaska Volcano Observatory

Different techniques, having different sensitivities, are being compared. Stereoscopic height retrievals based on MISR data effectively key on the layer of maximum spatial contrast, whereas other techniques are sensitive to other attributes of the aerosol or cloud vertical distribution. As such, the differences frequently provide additional information.

Redoubt Eruption – Alaska – April 5, 2009

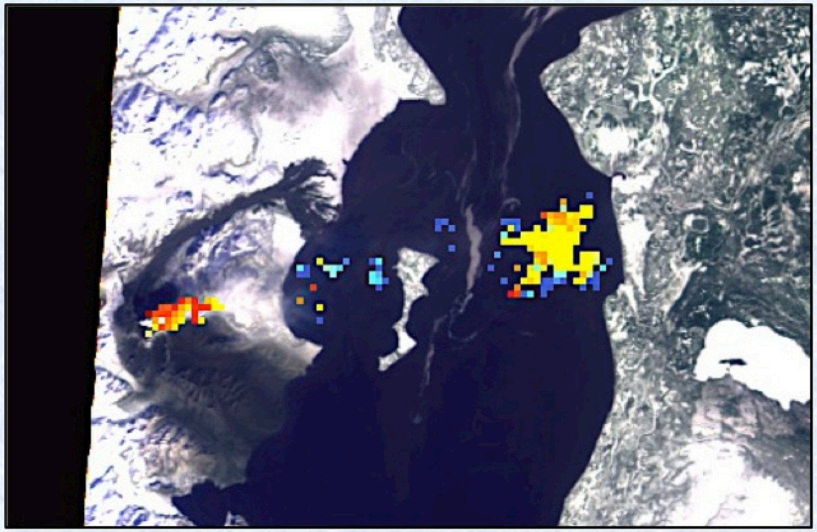

AVHRR retrieves heights near the water surface when the ash plume is thin

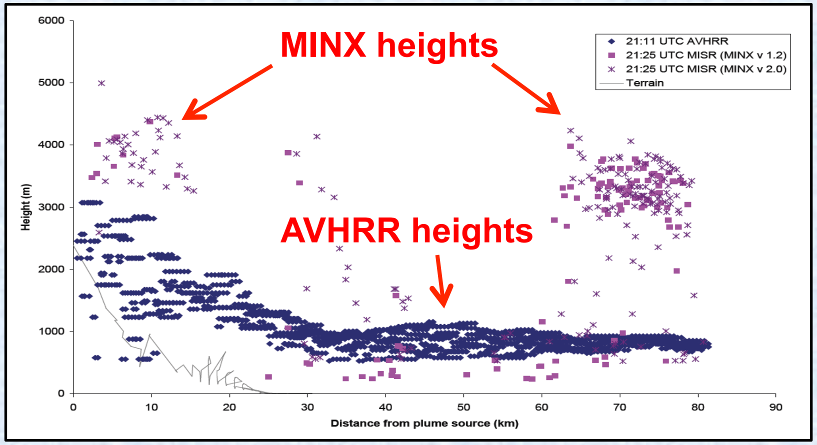

Images and analysis courtesy of Angela Ekstrand et al, AGU 2010

Height Retrieval Comparison – MINX and Micropulse Lidar

Collocation of micropulse lidar and MISR data at Anmyon on the coast of South Korea

by Ben Dunst, UCLA
and Mike Garay, JPL

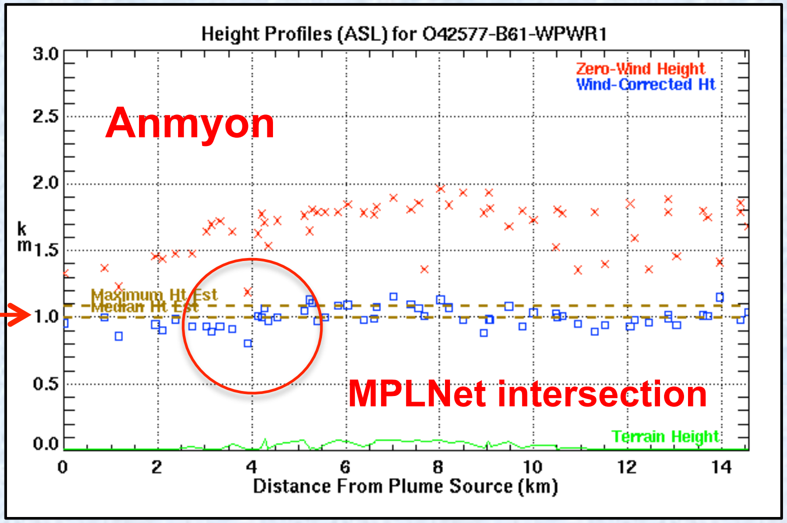

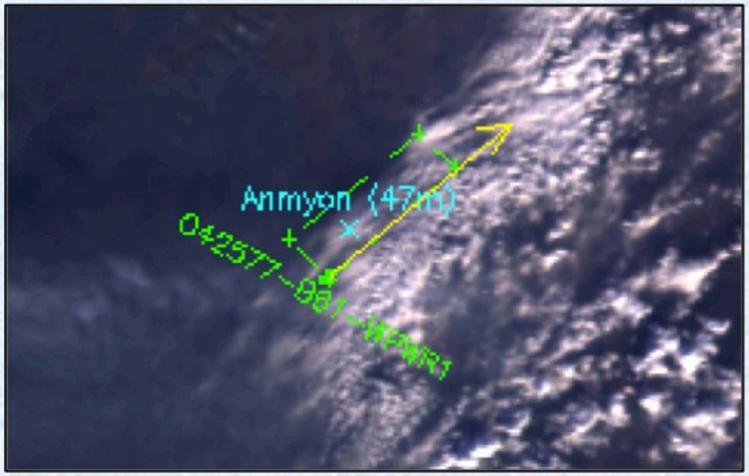

Wind direction for MINX retrieval derived from meteorological data

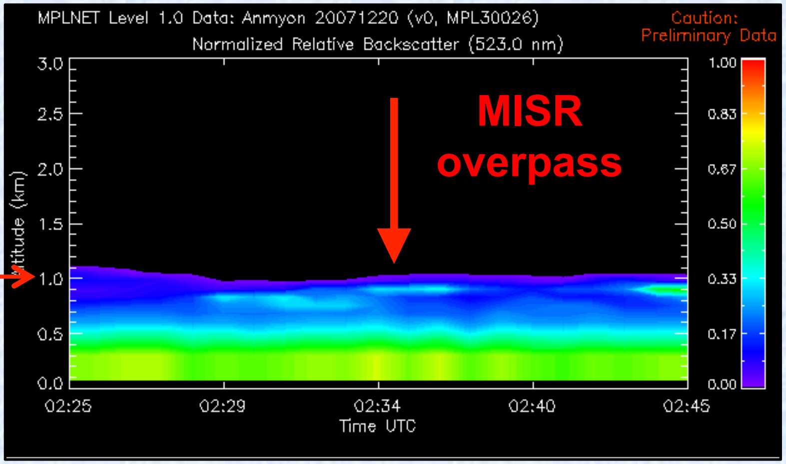

Height Retrieval Comparison – MINX and Calipso Lidar

Path 210

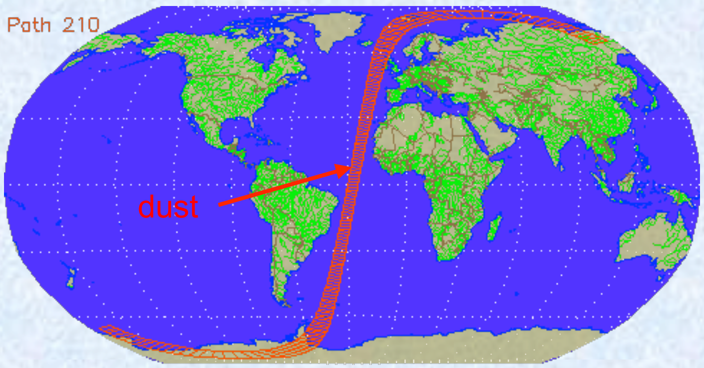

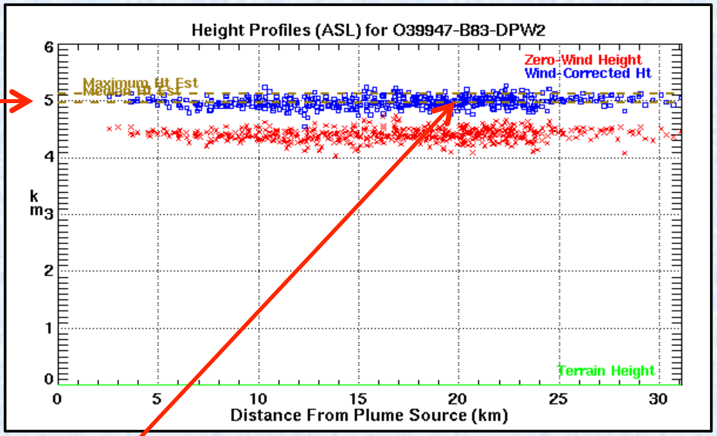

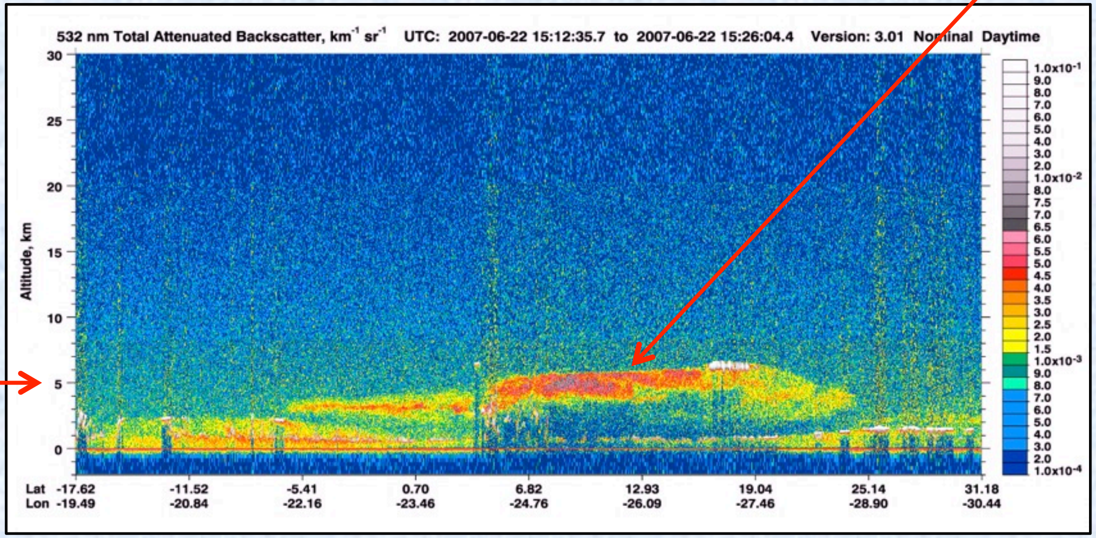

Dust over Atlantic Ocean off West Africa seen by Calipso lidar and MISR

by Olga Kalashnikova and Mark Chodas, JPL

Height Retrieval Comparison – MINX and Calipso Lidar

Biomass burning smoke over Borneo from 2001-2009 matches well with CALIPSO extinction profiles

by Michael Tosca, JPL (UCI)

Mean CALIPSO extinction

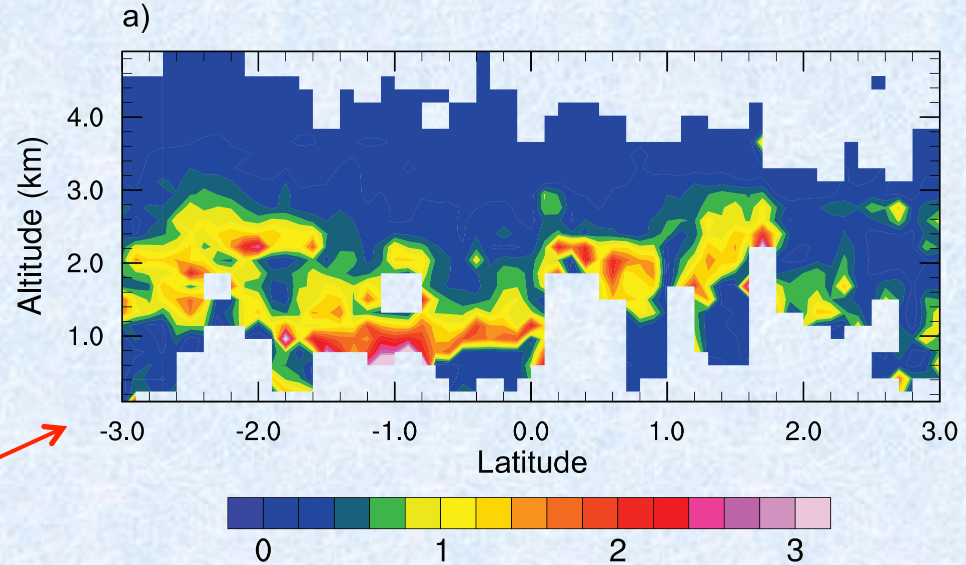

While CALIPSO sees thin smoke, the extinction weighted mean altitude matches very closely to the MISR mean smoke altitude as computed using MINX

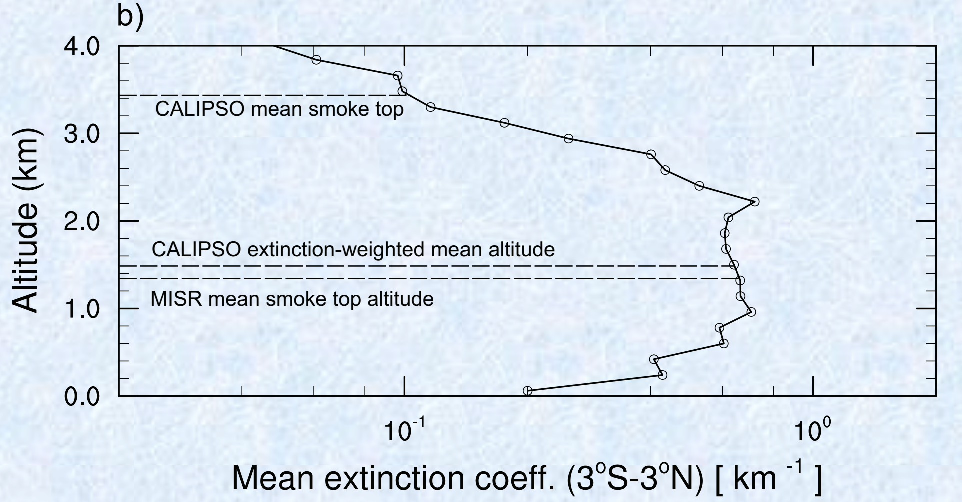

Height Retrieval Comparison – MINX and Calipso Lidar

Dust over Bodele Depression, Chad seen by Calipso lidar and MISR

by Mike Garay, JPL

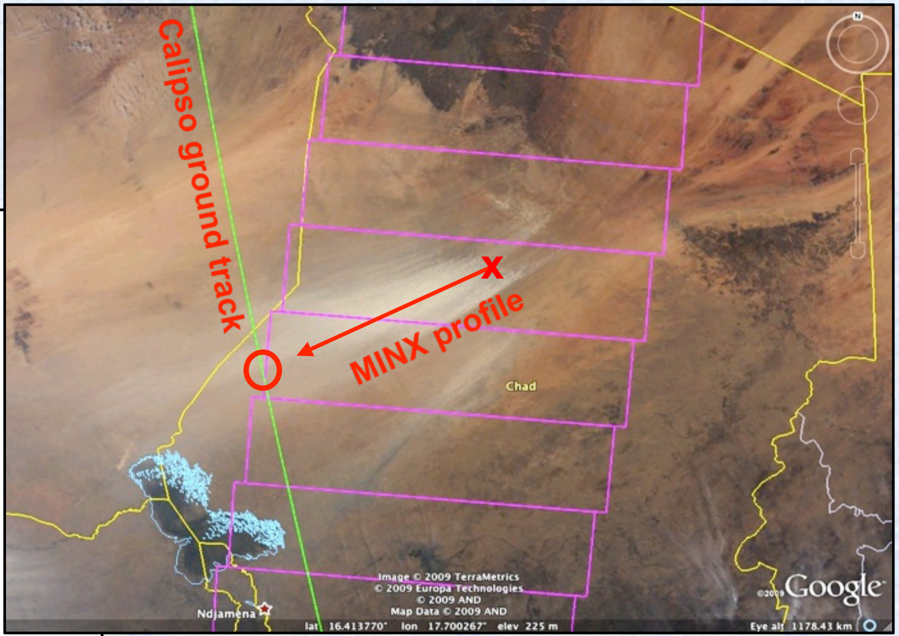

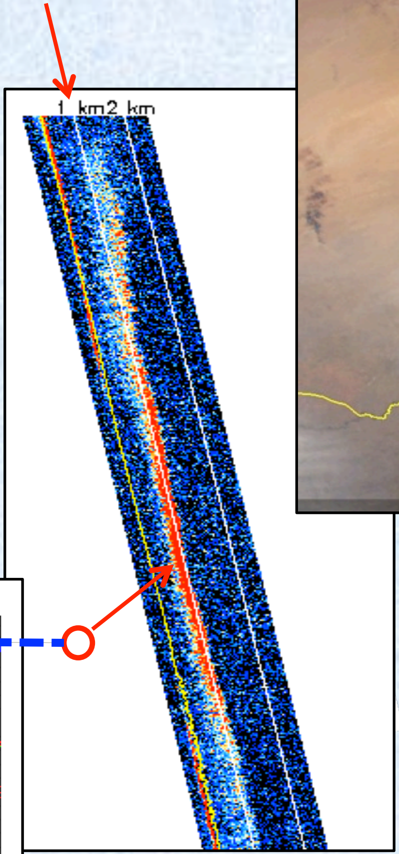

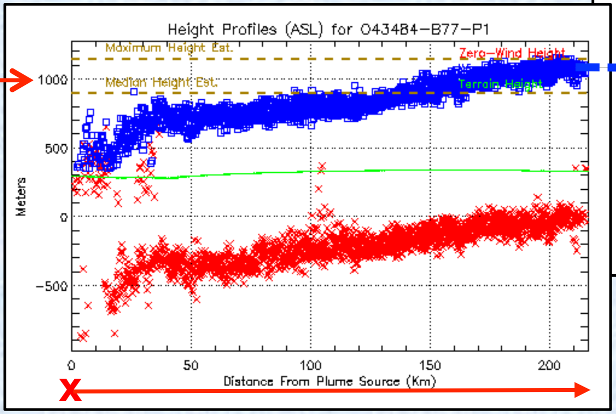

Path 183

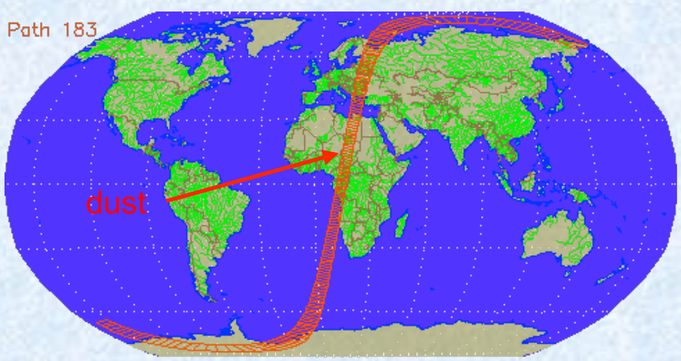

References

- Chen, Y., Q. Li, J.T. Randerson, E.A. Lyons, R.A. Kahn, D.L. Nelson, and D.J. Diner, 2009. The sensitivity of CO and aerosol transport to the temporal and vertical distribution of North American boreal fire emissions, Atm. Chem. Phys 9, 6559-6580.
- Diner, D.J., D.L. Nelson, Y. Chen, R.A. Kahn, J. Logan, F-Y. Leung, and M. Val Martin, 2008. Quantitative studies of wildfire smoke injection heights with the Terra Multi-angle Imaging SptectoRadiometer. SPIE Proceedings.
- Kahn, R., Y. Chen, D.L. Nelson, F-Y. Leung, Q. Li, D.J. Diner, and J.A. Logan, 2008. Wildfire smoke injection heights – Two perspectives from space, Geophys. Res. Lett. 35, doi:10.1029/2007GL032165.
- Kahn, R. A., W.-H. Li, C. Moroney, D. J. Diner, J. V. Martonchik, and E. Fishbein (2007). Aerosol source plume physical characteristics from space-based multiangle imaging, J. Geophys. Res., 112, D11205, doi:10.1029/2006JD007647.
- Mazzoni, D., J.A. Logan, D. Diner, R. Kahn, L. Tong, and Q. Li (2007). A data-mining approach to associating MISR smoke plume heights with MODIS fire measurements. Rem. Sens. Environ. 107, 138-148.
- Mims, S.R., R.A. Kahn, C.M. Moroney, B.J. Gaitley, D.L. Nelson, and M.J. Garay, 2009. MISR Stereo-heights of grassland fire smoke plumes in Australia. IEEE Trans. Geosci. Remt. Sens. 48, 25-35.
- Moroney, C., R. Davies, and J-P. Muller, 2002. MISR stereoscopic image matchers: Techniques and results, IEEE Trans. Geosci. Remt. Sens. 40, 1547-1559.
- Nelson, D. L., Y. Chen, R. A. Kahn, D. J. Diner, and D. Mazzoni, 2008. Example applications of the MISR INteractive eXplorer (MINX) software tool to wildfire smoke plume analyses. Proceedings of SPIE, 7089, 708909.1-708909.11.
- Sofiev, M., T. Ermakova, and R. Vankevich, 2012. Evaluation of the smoke-injection height from wild-land fires using remote-sensing data, Atmos. Chem. Phys., 12, 1995–2006, doi:10.5194/acp-12-1995-2012.
- Tosca, M.G., J.T. Randerson, C.S. Zender, D.L. Nelson, D.J. Diner, and J.A. Logan, 2011. Dynamics of fire plumes and smoke clouds associated with peat and deforestation fires in Indonesia, J. Geophys. Res., VOL. 116, D08207, 14 pp, doi: 10.1029/2010JD015148.
- Val Martin, M., J.A. Logan, R. Kahn, F-Y. Leung, D. Nelson, and D. Diner, 2010. Smoke injection heights from fires in North America: Analysis of five years of satellite observations, Atm. Chem. Phys. 10, 1491-1510.
- Wu, D.L., Diner, D.J., Garay, M.J., Jovanovic, V.M., Lee, J.N., Moroney, C.M., Mueller, K.J., and Nelson, D.L., 2010. MISR CMVs and Multiangular Views of Tropical Cyclone Inner-Core Dynamics, Proceeding of IWW10.
- Zong, J., R. Davies, J.P. Muller, and D.J. Diner, 2002. Photogrametric retrieval of cloud advection and top height from the multi-angle imaging spectroradiometer (MISR). Journal of the American Society for Photogrammetric Engineering and Remote Sensing, 68 (8), 821-830.